Published in final edited form as:
Oncogene. 2014 March 20; 33(12): 1538–1547. doi:10.1038/onc.2013.102.

Inactivation of TGF-β signaling and loss of *PTEN* cooperate to induce colon cancer *in vivo*

Ming Yu[1], **Patty Trobridge**, **Yuxin Wang**[2,3], **Samornmas Kanngurn**[1,4], **Shelli M. Morris**[1], **Sue Knoblaugh**[5], and **William M. Grady**[1,3]

[1]Clinical Research Division, Fred Hutchinson Cancer Research Center, Seattle, WA [2]Department of Microbiology, University of Washington, Seattle, WA [3]Department of Medicine, University of Washington, Medical School, Seattle, WA [4]Department of Pathology, Prince of Songkla University, Hatyai, Thailand [5]Comparative Medicine, Fred Hutchinson Cancer Research Center, Seattle, WA

Abstract

The accumulation of genetic and epigenetic alterations mediates colorectal cancer (CRC) formation by deregulating key signaling pathways in cancer cells. In CRC, one of the most commonly inactivated signaling pathways is the transforming growth factor-beta (TGF-β) signaling pathway, which is often inactivated by mutations of *TGF-β type II receptor* (*TGFBR2*). Another commonly deregulated pathway in CRC is the phosphoinositide-3-kinase (PI3K)-AKT pathway. Phosphatase and tensin homolog deleted on chromosome 10 (PTEN) is an important negative regulator of PI3K-AKT signaling and is silenced in approximately 30% of CRC. The combination of *TGFBR2* inactivation and loss of *PTEN* is particularly common in microsatellite unstable CRCs. Consequently, we determined *in vivo* if deregulation of these two pathways cooperate to affect CRC formation by analyzing tumors arising in mice that lack *Tgfbr2* and/or *Pten* specifically in the intestinal epithelium. We found that lack of *Tgfbr2* (*Tgfbr2*^{IEKO}) alone is not sufficient for intestinal tumor formation and lack of *Pten* (*Pten*^{IEKO}) alone had a weak effect on intestinal tumor induction. However, the combination of *Tgfbr2* inactivation with *Pten* loss (*Pten*^{IEKO};*Tgfbr2*^{IEKO}) led to malignant tumors in both the small intestine and colon in 86.0% of the mice and to metastases in 8.1% of the tumor-bearing mice. Moreover, these tumors arose via a β-catenin independent mechanism. Inactivation of Tgf-β signaling and loss of *Pten* led to increased cell proliferation, decreased apoptosis, and decreased expression of cyclin-dependent kinase inhibitors. Thus, inactivation of TGF-β signaling and loss of *PTEN* cooperate to drive intestinal cancer formation and progression by suppressing cell cycle inhibitors.

Keywords

colorectal cancer; transforming growth factor beta; PTEN; p21^{Cip1}; colon cancer

Introduction

Colorectal cancer (CRC) is one of the most commonly diagnosed malignancies in industrialized countries, and it remains the second leading cause of cancer-related deaths in the USA, accounting for 51,690 deaths during 2012.(1) Obtaining a better understanding of

Corresponding Author: William M. Grady, M.D., Fred Hutchinson Cancer Research Center, Clinical Research Division, 1100 Fairview Ave N., Mailstop D4-100, Seattle, WA 98109, Phone: 206-667-1107, Fax; 206-667-2917, wgrady@fhcrc.org.

Conflicts of Interest: No conflicts of interest exist for any of the authors.

the functionally significant genetic and epigenetic alterations that arise during the molecular pathogenesis of CRC will help lead to the development of more effective therapies for treating CRC.

The classic paradigm of CRC formation follows the adenoma→cancer sequence, in which CRC begins as a benign neoplasm, called an adenoma.(2) In this classic model, the adenomas are initiated by mutations that activate the Wnt signaling pathway (e.g. mutations in adenomatous polyposis coli (*APC)* or beta catenin (*CTNNB1*)).(3–5) Adenomas can then progress to malignancy if they acquire additional oncogenic mutations that lead to the deregulation of other pathways, such as the RAS-RAF-MAPK and/or the phosphoinositide-3-kinase (PI3K)-AKT signaling pathways.(6–8) It has also become clear that CRCs can be classified into three classes based on the form of genomic instability that they display: chromosomal instability (CIN), microsatellite instability (MSI), and CpG Island Methylator Phenotype (CIMP).(9) The Microsatellite Instability (MSI) class of CRC accounts for approximately 15% of CRC and results from inactivation of the DNA mismatch repair system. The MSI cancers often arise through a serrated polyp→cancer sequence.(10) They have a pronounced susceptibility to PI3K inhibitors compared to other CRCs, suggesting they are particularly dependent on the PI3K-AKT pathway.(11)

The PI3K-AKT signaling pathway is aberrantly activated in 40% of CRC.(7) Activation of PI3K signaling promotes cancer formation through a variety of mechanisms.(12–14) Phosphatase and tensin homologue deleted on chromosome 10 (PTEN) is an important negative regulator of PI3K-AKT signaling,(15) and its inactivation is a common cause of increased PI3K activity in cancers.(16) Loss of PTEN expression occurs in 20–40% of CRCs.(17, 18) and the MSI subtype has an especially high frequency of *PTEN* gene mutations compared to CIN CRC's.(19, 20) Notably, PTEN loss may also affect tumorigenesis through mechanisms other than PI3K pathway activation,(21) including the induction of genomic stability,(22) and deregulated cellular senescence.(23, 24)

Like the PI3K pathway, the TGF-β signaling pathway is commonly deregulated in human cancers.(25, 26) The importance of TGF-β signaling inactivation in CRC is highlighted by the high frequency of resistance to TGF-β, a multifunctional cytokine that acts as a tumor suppressor in the colon.(27) TGF-β mediates its effects on cells through a heteromeric cell surface receptor that consists of two obligate serine-threonine kinase components, TGF-β receptor type I (TGFBR1) and type II (TGFBR2). In colon cancer, the mutational inactivation of *TGFBR2* is a common mechanism for inactivating the TGF-β signaling pathway, especially in MSI CRCs.(28) Inactivation of *TGFBR2* can result in the deregulation of a multitude of cellular processes that may affect tumorigenesis.(29, 30) The myriad of cellular processes that can be affected by TGF-β signaling inactivation raises the question of which ones are functionally relevant for CRC formation. Furthermore, the effects of TGF-β signaling deregulation in CRC appear to depend on the concurrent signaling pathways that are altered in the cancer cells.(31, 32) Indeed, it is increasingly appreciated that the TGF-β signaling pathway interacts intimately with a variety of pathways including the Wnt-APC-β-catenin, RAS-RAF-MAPK, and PI3K-AKT pathways, and that the interaction of these pathways may be a major factor that determines the biological consequences of TGF-β signaling inactivation in CRC cells.(33, 34)

In light of the common co-occurrence of mutations in *TGFBR2* and *PTEN* in CRC, especially in MSI CRC, we generated an *in vivo* model to directly assess whether these genetic alterations cooperate in intestinal cancer formation. We found that inactivation of *Tgfbr2* and loss of *Pten* converge to suppress cyclin dependent kinase inhibitors, which may promote intestinal cancer formation and progression *in vivo*.

Results

Inactivation of *Tgfbr2* alone or loss of *Pten* alone has little to no effect on tumor formation in the intestinal epithelium

In order to assess the *in vivo* effects of TGF-β signaling inactivation and PI3K-AKT signaling deregulation on intestinal tumorigenesis, *Villin-Cre* transgenic mice were bred with mice carrying $Pten^{flx/flx}$ and $Tgfbr2^{flx/flx}$ alleles to create three cohorts of mice: *Villin-Cre;*$Tgfbr2^{flx/flx}$ (no *Tgfbr2* in the intestinal epithelium, designated $Tgfbr2^{IEKO}$); *Villin-Cre;*$Pten^{flx/flx}$ (no *Pten* in the intestinal epithelium, designated $Pten^{IKEO}$) and *Villin-Cre;*$Pten^{flx/flx}$;$Tgfbr2^{flx/flx}$ (no *Pten* and no *Tgfbr2* in the intestinal epithelium, designated $Pten^{IKEO}$;$Tgfbr2^{IEKO}$). No intestinal tumors were observed in the control mice lacking *Villin-Cre* (Control). Consistent with previous studies, mice that lacked *Tgfbr2* in the intestinal epithelium did not develop tumors by 54 weeks of age. This observation supports our previous studies, suggesting that inactivation of TGF-β signaling alone is not sufficient for intestinal tumor formation.(31, 33)

Deletion of *Pten* in the intestinal epithelium of $Pten^{IKEO}$ mice was confirmed by immunohistochemistry (IHC) using an antibody specific for PTEN (Supplemental Figure S4). $Pten^{IKEO}$ mice (N=39) were necropsied and examined as noted in the Methods section. The majority of *Pten*-deficient mice did not have gross or microscopic abnormalities in their intestinal epithelium, which is similar to the findings of Marsh et al and Byun et al. (35, 36) However, unlike in the published studies, we did find gross lesions in 3 $Pten^{IKEO}$ mice (Table 1). These lesions varied from mild hyperplasia (small intestine and cecum) to a single adenocarcinoma (small intestine), which was characterized by dysplastic glands invading into the muscularis propria. There were no large mucinous adenocarcinomas found in the $Pten^{IKEO}$ mice.

Tgfbr2 inactivation in the context of *Pten* loss promotes intestinal tumor formation

The inactivation of *TGFBR2* and loss of *PTEN* are common concurrent molecular events observed in CRC, raising the possibility that deregulation of these pathways may cooperate to promote the formation of intestinal cancer.(19, 20, 37) This possibility led us to generate mice that were deficient for both *Pten* and *Tgfbr2* in the intestinal epithelium ($Pten^{IEKO}$;$Tgfbr2^{IEKO}$). *Tgfbr2* inactivation in the context of *Pten* loss significantly shortened the life span of these mice to a median survival of 36 weeks (Figure 1, $Pten^{IEKO}$;$Tgfbr2^{IEKO}$ mice compared to $Tgfbr2^{IEKO}$ mice, $Pten^{IEKO}$ mice or Control mice, $P < 0.0001$ for all comparisons). A majority of $Pten^{IEKO}$; $Tgfbr2^{IEKO}$ mice (N=37/43) developed gross lesions, a significant increase in the number of tumor-bearing $Pten^{IEKO}$;$Tgfbr2^{IEKO}$ mice as compared to $Tgfbr2^{IEKO}$ mice, $Pten^{IEKO}$ mice or Control mice (Table 1, $P < 0.0001$ for all comparisons). A total of 49 adenocarcinomas in $Pten^{IEKO}$; $Tgfbr2^{IEKO}$ mice were confirmed by pathology. The majority of tumors were mucinous adenocarcinomas with transmural effacement by neoplastic glands and large lakes of tumor-produced mucin. In some cases, mucin lakes extended through the serosa and into the serosal lymphatics. (Figure 2A) Mucinous adenocarcinomas occurred in the small intestine (N=16, 32.7%), cecum (N=11, 22.4%), colon (N=13, 26.5%), and cecal junctions (N=9, 18.4%). (Table 2) Alcian blue staining further confirmed mucin production in the adenocarcinomas (Supplemental Figure S1). Confirmation of the expected gene status of the normal intestinal mucosa and tumors of the various genotypes was carried out using PCR-based assays that assess for cre-mediated recombination of the floxed alleles. (Supplemental Figure S2) (33, 38)

Notably, 8.1% of the tumor-bearing $Pten^{IEKO}$;$Tgfbr2^{IEKO}$ mice were found to have metastases within the adjacent mesentery, pancreas, and peritoneal cavity (body wall, uterus,

and prostate). A single mouse did have metastasis to the liver with intravascular neoplastic cells. (Figure 2B–C) Thus, metastases were confirmed histologically and appeared to occur both via intravascular and transcoelomic routes. The metastases were also assessed with Alcian blue staining, E-cadherin immunostaining, and by PCR for the recombined *Tgfbr2*^{flx} alleles to confirm that they were derived from the primary mucinous adenocarcinomas. (Figure 2D–F)

Thus, inactivation of *Tgfbr2* with loss of *Pten* in the intestinal epithelium results in the formation of adenocarcinomas in the small intestine, cecum, and colon. The presence of metastases in some of the mice suggests that loss of TGF-β signaling contributes to ametastatic phenotype in the context of *Pten* loss.(39)

Signaling pathway deregulation in the tumors arising in the *Pten*^{IEKO}*;Tgfbr2*^{IEKO} mice

We first confirmed that the neoplastic cells in the *Pten*^{IEKO}*;Tgfbr2*^{IEKO} mice did not express *Pten* by IHC. (Figure 3B) Since PTEN exerts tumor suppressive functions by inhibiting the PI3K-AKT pathway, we analyzed the activation status of the PI3K-AKT pathway by IHC using antibodies specific for phospho-AKT Serine 473 (Ser473). We observed neoplastic epithelial cells in *Pten*^{IEKO}*;Tgfbr2*^{IEKO} mice had increased nuclear phosphorylated Akt Ser473 compared to the normal intestinal epithelium. (Figure 3C)

Next, we assessed the phosphorylation status of Akt at both Thr308 and Ser473 in the normal intestinal mucosa and tumors of the mice by immunoblotting. (Figure 3E) We detected total Akt but not phospho-Akt in the normal mucosa of the wild-type control mice, which is consistent with previous reports.(35) Of interest, a modest increase in phospho-Akt (Ser473), but not Thr308, was detected in the normal mucosa of the *Tgfbr2*^{IEKO} mice, indicating that inactivation of TGF-β signaling leads to phosphorylation of Akt at Ser473 in the setting of intact *Pten*. This is presumably secondary to indirect effects of loss of Tgfbr2 and was unexpected in light of prior studies in epithelial cells that showed that TGF-β signaling can induce Akt phosphorylation at Ser473.(40) Increased Akt phosphorylation levels at both Thr308 and Ser473 sites were observed in the normal mucosa of *Pten*-deficient mice compared to wild-type mice. However, we observed less phosphorylated Akt in the tumors from the *Pten*^{IEKO}*;Tgfbr2*^{IEKO} mice compared to the normal mucosa, even though total Akt levels were increased in the tumors. (Figure 3E, right panel) These results raise the possibility of negative feedback regulation occurring in the tumors and suggest that a reduction in PI3K activity is selected for during intestinal cancer formation.

We also assessed the activation status of the MAPK signaling pathway in the normal intestinal mucosa and tumors because this signaling pathway is often induced in human CRC and can be regulated by TGF-β.(41) We found that the MAPK pathway, as measured by phospho-ERK1/2, was activated at a basal state of the normal mucosa of the control mice and the *Tgfbr2*^{IEKO} mice. (Figure 3F, left panel) In contrast to increased Akt phosphorylation, less MAPK activation was observed in the majority of normal mucosa samples of the Pten-deficient mice, regardless of the*Tgfbr2* status, and there was also more inter-individual variation in the *Pten*^{IEKO} mice compared to the control mice. (Figure 3F, right panel) Despite there being less ERK activation in the normal intestines of the mice lacking *Pten*, we observed increased ERK1/2 phosphorylation in the tumors when compared to normal mucosa in the *Pten*^{IEKO}*;Tgfbr2*^{IEKO} mice, indicating that the MAPK pathway is upregulated in the *Pten*^{IEKO};*Tgfbr2*^{IEKO} tumors. To determine if somatic oncogenic *Kras* mutations are responsible for the increased MAPK pathway activation in the tumors from the *Pten*^{IEKO}*;Tgfbr2*^{IEKO} mice, we sequenced the tumors for *Kras* mutations. However, we did not detect mutations in *Kras* (codons 12, 13 or 61) in any of *Pten*^{IEKO}*;Tgfbr2*^{IEKO} tumors assayed (N=5).

The intestinal tumors in the *Pten^{IEKO};Tgfbr2^{IEKO}* mice arise independently of the canonical Wnt-β-catenin pathway

Given the high frequency of *APC* and *CTNNB1* mutations and subsequent Wnt pathway activation in human CRC and the fact that loss of *Tgfbr2* or *Pten* alone does not appear to be sufficient to initiate intestinal tumor formation,(26) we assessed the activation state of the Wnt signaling pathway in the tumors arising in the *Pten^{IEKO};Tgfbr2^{IEKO}* mice. In addition, the Wnt pathway was of interest in light of conflicting data regarding its role in initiating tumor formation in the setting of *Pten* deficiency.(35, 36, 42, 43) The activation state of the Wnt signaling pathway was assessed by determining the nuclear localization status of β-catenin. (Figure 3D) The membrane-bound localization of β-catenin was observed in 75% of the *Pten^{IEKO}* tumors analyzed (N=4) and in 100% of the *Pten^{IEKO};Tgfbr2^{IEKO}* tumors analyzed (N=10). We only observed nuclear localization of β-catenin in one adenoma from a *Pten^{IEKO}* mouse (Supplemental Figure S4), which we presume was secondary to a somatic event in the tumor with subsequent activation of Wnt signaling. We also analyzed the levels of Wnt target genes, *Axin2* and *Cd44*, by qRT-PCR.(44–46) We did not observe a significant up-regulation of these Wnt target genes in the tumors arising in *Pten^{IEKO};Tgfbr2^{IEKO}* mice as compared to the normal intestinal epithelial tissue from the *Pten^{IEKO}*, *Tgfbr2^{IEKO}* or *Pten^{IEKO};Tgfbr2^{IEKO}* mice. ($P = 0.45$ for *Axin2;* $P = 0.33$ for *Cd44*, Supplemental Figure S5) Overall, these results suggest that the canonical Wnt-β-catenin pathway is not activated in these mice.

Inactivation of *Tgfbr2* and *Pten* loss do not cooperate to induce tumor formation through effects on genomic stability

Both PTEN and TGF-β signaling have been implicated in the control of genomic stability.(47) Thus, we assessed the tumors for aneuploidy using microarray comparative genomic hybridization (array CGH) (N=3). However, we found no chromosomal gains or losses in the tumors. (Supplemental Figure S6) These results demonstrate that these tumors do not have gross chromosomal abnormalities representative of chromosomal instability and also do not reveal a common locus that is altered somatically in the tumors. The identification of a commonly deleted or amplified locus would have indicated a possible somatic event that was cooperating with loss of TGFBR2 and PTEN to drive tumor formation in the *Pten^{IEKO};Tgfbr2^{IEKO}* mice.

Deregulation of cell cycle control proteins in *Pten^{IEKO};Tgfbr2^{IEKO}* mouse tumors

In light of the increased MAPK pathway signaling in the *Pten^{IEKO};Tgfbr2^{IEKO}* tumors, we assessed tumor cell proliferation (by Ki-67 immunostaining) to determine if enhanced proliferation is one of the biological effects driving tumor formation in the *Pten^{IEKO};Tgfbr2^{IEKO}* mice. (Figure 4A) We observed that a substantial portion of the neoplastic cells in the *Pten^{IEKO};Tgfbr2^{IEKO}* mice were positive for Ki67 staining (average percent positive cells/tumor = 50.0% ± 26%). As both PI3K-AKT and TGF-β pathways have been implicated in the induction of apoptosis, we also assessed apoptosis in tumors from the *Pten^{IEKO}* and *Pten^{IEKO};Tgfbr2^{IEKO}* mice by cleaved caspase-3 immunostaining. (Figure 4B) We found neoplastic glands in the *Pten^{IEKO};Tgfbr2^{IEKO}* mice had very little cleaved caspase-3 staining. We also assessed cleaved caspase-3 by immunoblotting and observed decreased cleaved caspase-3 protein level in the tumors arising in the *Pten^{IEKO};Tgfbr2^{IEKO}* mice compared to the normal mucosa in the other mouse cohorts. (Supplemental Figure S7) These results suggest that increased proliferation and decreased apoptosis contribute to the formation of the tumors in the *Pten^{IEKO};Tgfbr2^{IEKO}* mice.

Cyclin dependent kinase (CDK) inhibitors $p15^{INK4B}$, $p21^{CIP1}$ and $p27^{KIP1}$ are well-documented target genes of the TGF-β signaling pathways.(48–50) They play an essential role in the control of the cell cycle and proliferation and their expression is often decreased

in cancer.(51–53) Therefore, we assessed the levels of *Cdkn2b/p15*^{Ink4b}, *Cdkn1a/p21*^{Cip1} and *Cdkn1b/p27*^{Kip1} mRNA by qRT-PCR in the matched normal and tumor tissue. (Figure 4C) Expression of all three CDK inhibitors genes was significantly lower in the tumor samples compared to the matched normal epithelium (for all comparisons, $P < 0.02$). Furthermore, we analyzed the protein levels by immunoblot. (Figure 4D) Expression of p15^{Ink4b}, p21^{Cip1} and p27^{Kip1} proteins was detected in the normal mucosa of various genotypes regardless of *Pten* and *Tgfbr2* status. Comparison of protein levels between normal and tumor tissue from *Pten*^{IEKO}*;Tgfbr2*^{IEKO} mice revealed significantly decreased expression of p15^{INK4B}, p21^{Cip1} and p27^{Kip1} in the tumor tissue (T) compared to normal tissue (N) (* $P < 0.05$, Mann-Whitney test, N=3). These results reveal a marked decrease in expression of CDK inhibitors in tumors, suggesting this is a tumor-promoting biological consequence resulting from the cooperation of inactivation of *Tgfbr2* and loss of *Pten*.

Reconstitution of PTEN and TGFBR2 cooperate to induce *p21*^{Cip1} expression in human colon cancer cells

In order to assess the causal role of PTEN and TGFBR2 in the regulation of the CDK inhibitors, we reconstituted *PTEN* and/or *TGFBR2* in the SNU-C4 colon cancer cell line, a human CRC cell line with both mutant *PTEN* and *TGFBR2*.(54) We then evaluated the SNU-C4 cells for *p21*^{CIP1} promoter activation using the p21Pδ2.1-luc reporter, a *p21*^{CIP1} promoter containing the minimal TGF-β response elements (55). As shown in Figure 5, reconstitution of *TGFBR2* in SNU-C4 cells induced expression of the p21Pδ2.1-luc reporter by 4-fold compared to control vector. Similarly, reconstitution of *PTEN* alone induced a 3-fold increase in luciferase activity. Reconstitution with both wild-type *TGFBR2* and *PTEN* further induced the expression of p21Pδ2.1-luc by 10-fold. To confirm the specificity of the cooperation between *TGFBR2* and *PTEN* on the transcriptional activation of *p21*^{CIP1}, we assessed the effect of reconstituted *PTEN* and *TGFBR2* on activating the 3TP-lux luciferase reporter, which assesses TGF-β pathway activation. Reconstitution of the SNU-C4 cells with *PTEN* alone did not induce 3TP-lux activity. (Figure 5, Supplemental Figure S8) Furthermore, there was no further increase in the luciferase activity of the 3TP-lux reporter in *TGFBR2* and *PTEN* co-transfected cells compared to *TGFBR2*-transfected alone cells, indicating the additive effect of *PTEN* and *TGFBR2* on *p21*^{CIP1} transcription activation is specific for *p21*^{CIP1}. These results suggest deregulated cell cycle proteins are likely downstream mediators through which inactivation of *TGFBR2* and loss of *PTEN* cooperate to promote tumor formation and progression.

Discussion

It is widely appreciated that the majority of CRC develop as a consequence of the progressive accumulation of genetic and epigenetic alterations in evolving clones of tumor cells.(9) The Cancer Genome Atlas Network (TCGA) recently completed whole exome sequencing of 224 CRCs and found components in the TGF-β and PTEN/PI3K/AKT pathways were frequent mutational targets.(26) A major challenge emerging from cancer genome sequencing projects, like the TCGA study described above, is how to determine which of the mutations found in the tumors are “drivers” of cancer formation and which are “passengers”. Some of these mutations have been studied in cancer cell lines, but their relevance to *in vivo* tumor initiation and progression is not clear. Consequently, we generated the *Pten*^{IEKO}*;Tgfbr2*^{IEKO} mice to study the effect of deregulation of these two pathways on cancer formation *in vivo.*

Deregulation of the PTEN/PI3K-AKT pathway has been associated with the growth and progression of CRC.(56, 57) Loss of PTEN appears to be the most common mechanism for deregulating the PI3K pathway, but little is known regarding the specific mechanisms

through which PTEN loss mediates its effects *in vivo* on colon cancer formation. Our studies and previously published studies now identify potential functional consequences of loss of *PTEN* in driving tumor formation in the intestines, and demonstrate the importance of gene cooperation in the formation of CRC. (35, 42, 58) Using mice that lack *Pten* in the intestinal epithelium, we found phosphorylation of Akt at both Ser473 and Thr308 was increased in the normal intestinal epithelial cells of *Pten*-deficient mice. This finding is consistent with the role of *PTEN* as a negative regulator of PI3K-AKT activity.(15, 59) However, the loss of *PTEN* alone had weak tumor promoting effects in the intestines, which suggests that for effective tumorigenesis, deregulation of the PI3K pathway requires the cooperation of other deregulated pathways. Our results differ from those of a recent published study in which mice expressing a dominantly active *Pik3ca* transgene spontaneously developed metastatic intestinal cancer.(60) Potential explanations for the common spontaneous development of tumors in their mouse model are the use of the *Pi3kca** transgene, which is a dominant active form of *Pi3kca p110α,* and the use of mice in a different genetic background than the mice in our studies.

In light of the modest effect of PTEN loss on intestinal tumor formation and because mutational inactivation of *TGFBR2* is often concurrent with loss of PTEN in human CRC(9), we proposed that the TGF-β and PI3K pathways may cooperate to drive CRC formation. The results of this study in which we observed a substantial increase in adenocarcinoma formation in mice lacking both *Pten* and *Tgfbr2* provide support for this idea. However, it is worth noting that the majority of tumor-bearing mice developed 1–2 adenocarcinoma, indicating low tumor multiplicity in these mice. Therefore, we propose that additional cooperating events are needed for the initiation of intestinal tumors in the $Pten^{IEKO};Tgfbr2^{IEKO}$ mice. Along these lines, it is interesting that there is no evidence of Wnt pathway activation in the tumors in this mouse model. The recently identified "hypermutated class" of CRCs found by TCGA also often lack *APC* mutations(26), which raises the possibility that the $Pten^{IEKO};Tgfbr2^{IEKO}$ mouse model may recapitulate features of this newly described class of CRC. Further studies of this class of human CRC may provide insight into the nature of the additional somatic events occurring in the $Pten^{IEKO};Tgfbr2^{IEKO}$ mouse tumors and will also allow a determination of how well the $Pten^{IEKO};Tgfbr2^{IEKO}$ mice model the hypermutated class of CRC.

After observing cooperation between inactivation of *Tgfbr2* and loss of *Pten* on intestinal tumor formation, we investigated potential mechanisms that could be driving this effect. One potential mechanism revealed by our studies is the deregulation of CDK inhibitor expression. Inactivation of *Tgfbr2* and *Pten* loss resulted in marked suppression of cyclin dependent kinase inhibitors in the tumor cells. Consistent with loss of CDK inhibitor expression, we observed increased proliferation in these tumors, which has also been observed in MSI CRCs.(61) These results suggest that inhibition of CRC development by *PTEN* and *TGFBR2* is due in part to the collaborative regulation of cell cycle proteins. Consistent with this possibility, we observed that reconstitution of PTEN and TGFBR2 had an additive effect on inducing $p21^{CIP1}$ expression in human cancer cells.

Our studies suggest that the loss of CDK inhibitors is a significant mechanism through which PTEN and TGFBR2 inactivation promotes intestinal cancer formation. We have not yet identified a mechanism through which inactivation of *Tgfbr2* and loss of *Pten* may be affecting expression of CDK inhibitors, but candidate mechanisms include alterations in *Pik3r1* activity or in activin signaling.(56, 62–65) Furthermore, there are additional candidate biological effects through which Tgfbr2 inactivation and PTEN loss may promote intestinal tumor formation. For instance, we observed the loss of senescence markers $p19^{Arf}$ and Dcr2 in $Pten^{IEKO};Tgfbr2^{IEKO}$ tumors. (Supplemental Figure S9) Senescence functions as a barrier to oppose tumorigenesis and can be triggered by a variety of mechanisms

including the activation of oncogenic pathways or the loss of *PTEN*.(66–68) AKT activation has been shown to induce senescence through mechanisms involving $p27^{Kip1}$ in prostate cancer.(69) Thus, it is possible that *Tgfbr2* inactivation may help tumor cells escape *Pten*-loss induced senescence, which could be another cooperative mechanism that drives the tumor progression in the $Pten^{IEKO};Tgfbr2^{IEKO}$ mice. Further studies are needed to assess this possibility.

In summary, we have generated an *in vivo* mouse model to assess whether cooperation between two frequent events found in human colon cancer, *TGFBR2* mutations and PTEN loss, plays a functional role in the molecular pathogenesis of CRC. Our results provide evidence that the cooperative interactions between inactivation of TGFBR2 and loss of *PTEN* converge on deregulating CDK inhibitors to promote tumorigenesis in CRC. These findings raise the possibility that agents targeted at the cyclin:CDK enzyme complexes may be particularly effective in CRCs that carry *TGFBR2* mutations and lack *PTEN* expression. Furthermore, our mouse model recapitulates molecular features seen in a subset of CRC ("hypermutated class" of CRC) and has the potential for use as a pre-clinical model for CRC to test novel therapeutic targets.

Materials and Methods

Generation and characterization of *Villin*-Cre; $Pten^{flx/flx};Tgfbr2^{flx/flx}$ mice

The generation of the following genetically engineered mice has been previously described: *Villin*-Cre;$Tgfbr2^{flx/flx}$ ($Tgfbr2^{IEKO}$) and $Pten^{flx/flx}$ (33, 38). The $Tgfbr2^{IEKO}$ and $Pten^{flx/flx}$ mice were mated to generate the following genotypes: *Villin*-Cre; $Pten^{flx/flx};Tgfbr2^{wt/wt}$ ($Pten^{IEKO}$), and *Villin*-Cre;$Pten^{flx/flx};Tgfbr2^{flx/flx}$ ($Pten^{IEKO};Tgfbr2^{IEKO}$). The floxed *Tgfbr2* ($Tgfbr2^{flx/flx}$) and Villin-Cre mice were maintained on C57BL/6J background. Prior to generating the mice with the multiple mutant genotypes, $Pten^{flx/flx}$ mice were backcrossed onto a C57BL/6J background for at least five generations to obtain mice that are >90% C57BL/6J. Thus, the background strain of experimental mice was predominantly C57BL/6J with a small proportion of 129Sv. Mice were fed *ad libitum* with a standard rodent diet. Mice were harvested at 54 weeks of age, or earlier if moribund. The studies were approved by the local IACUC.

Mouse tissue processing

Mouse tissues were handled as previously described.(33, 34). Briefly, the small intestine, cecum, and colon were removed, opened, flushed with cold PBS and then examined grossly for tumors. Grossly visible tumors were measured and collected for histopathology. All major organs were examined for gross lesions, and mesenteric lymph nodes, lungs, liver were collected and evaluated histologically in all the mice. Gross lesions suspected to be metastases were confirmed histologically by S.K. The tissues were either snap-frozen in liquid nitrogen and stored at −80 C for RNA and protein extractions or fixed in 10% neutral buffered formalin (Fisher Scientific, Pittsburgh, PA) for 3–7 days, transferred to 70% ethanol, embedded in paraffin, and cut into 4 μm sections for H&E staining or immunostaining.

Immunoblotting

Protein lysates were obtained using standard methods and then resolved by SDS-PAGE gels and transferred to PVDF membranes (Thermo Scientific, Rockford, IL). Densitometric quantification of immunoblots was performed using the ImageJ 1.43 software. The following primary antibodies were used: rabbit anti-p44/42 total MAPK (ERK1/2) (1:1000, #9102 Cell Signaling, Danvers, MA), rabbit anti-phospho-p44/42 MAPK (phospho-ERK1/2) (Thr202/Tyr204, 1:2000, #4370 Cell Signaling), rabbit anti-pAKT (Ser473,

1:1,000, #9271 Cell Signaling), rabbit anti-pAKT (Thr308, 1:1,000, #9275 Cell Signaling), rabbit anti-total AKT(1:1,000, #9297 Cell Signaling), rabbit $p15^{INK4B}$ (1:1,000, #4822 Cell Signaling), rabbit $p21^{Cip1}$ (1:1,000, SC-469 Santa Cruz Biotechnology, Santa Cruz, CA), rabbit anti-$p27^{Kip1}$ (1:1,000, kindly provided by Dr. Matthew Fero), rabbit anti-$p19^{Arf}$ (1:1,000, PC435 Calbiochem®, EMD Biosciences, Billerica, MA), rabbit anti-Dcr2 (1:1,000, Ab2019, Abcam, Cambridge, MA), goat anti-β-Actin (1:5,000, SC-1616 Santa Cruz Biotechnology). The following secondary antibodies were used: goat anti-rabbit IgG-HRP (1:5,000, #SC-2004, Santa Cruz Biotechnology), donkey anti-goat IgG-HRP (1:5,000, #SC-2020, Santa Cruz Biotechnology).

Immunohistochemistry (IHC) staining

Hemotoxylin and Eosin (H&E) and Alcian blue staining, Ki67, β-catenin, and E-cadherin immunohistochemical assays were performed in the Experimental Histopathology Core at the Fred Hutchinson Cancer Research Center following routine laboratory protocol. Specific protocols are available upon request.

Comparative genomic hybridization

Acquired gains and losses of chromosomal material were assessed by microarray comparative genomic hybridization (array CGH). Three tumors from three individual mice were analyzed. Matched non-neoplastic reference DNA was obtained from the spleen from each mouse to minimize detection of constitutional copy number variants. Analysis was performed as previously described.(34)

Sequencing analysis of *Kras* gene mutation

Genomic DNA was isolated from normal intestinal mucosa and tumors using DNeasy Blood & Tissue Kit (Qiagen, Valencia, CA) according to the manufacturer's instructions. Amplification of *Kras* exon1&2 was performed by polymerase chain reaction (PCR) as previously described.(70)

Real-time quantitative reverse transcription polymerase chain reaction (qRT-PCR)

mRNA was extracted from snap-frozen tissues using TRIzol (Life Technologies, Grand Island, NY) following the manufacturer's instructions. cDNA was generated using standard procedures using oligodT primers (Life Technologies). TaqMan gene expression assays (Assays-on-Demand; Applied Biosystems, Foster City, CA) for $p15^{Ink4b}$ (*Cdkn2b*, Mm00483241_m1), $p21^{Cip1}$ (*Cdkn1a*, Mm00432448_m1), $p27^{Kip1}$(*Cdkn1b*, Mm00438168_m1) and β-glucuronidase (Gusb, Mm01197698_m1) were used for qRT-PCR. The assays were performed using the Bio-Rad CFX96 real-time PCR systems (Bio-Rad, Hercules, CA). The results of the qRT-PCR assays were normalized to β-glucuronidase (Gusb). Statistical analysis was performed using the GraphPad Prism version 4.00 software. The Mann-Whitney test was used for comparisons of quantitative results from the qRT-PCR assays. A P value of <0.05 was regarded as significant.

Tissue culture

The human colon cancer cell line SNU-C4 was generously provided by the Korean Cell Line Bank (Dr. Ja-Lok Ku, Seoul, Korea) and grown in RPMI 1640 (Life Technologies) supplemented with 10% FBS (HyClone, Logan, UT).

Plasmid transfection experiments

Transfections were performed using FuGene9 (Roche, Indianapolis, IN) following the manufacturer's protocol. The pCMV5-TGFBR2 expression vector, which carries HA tagged

wild-type *TGFBR2*, was kindly provided by Joan Massagué (Memorial Sloan-Kettering Cancer Center, New York, NY). An expression vector containing the human *PTEN* open reading frame pORF9-hPTEN was purchased from Invivo Gen (San Diego, CA).

Luciferase reporter assay

SNU-C4 cells were transiently transfected with the p21Pδ2.1 reporter (kindly provided by Xiaofan Wang, Duke University, Durham, NC) or p3TP-lux reporter (kindly provided by Joan Massagué, Memorial Sloan-Kettering Cancer Center, New York, NY) concomitantly with the pRL-TK reporter construct (Promega, Madison, WI), which expresses *Renilla* luciferase. Subsequently, the cells were treated with TGF-β1 (2 ng/ml), and luciferase activity was evaluated 48h after transfection using the Dual Luciferase Reporter Assay System (Promega) with a Veritas luminometer (Turner Biosystems, Sunnyvale, CA). Luciferase activities were normalized based on *Renilla* luciferase activity.

Supplementary Material

Refer to Web version on PubMed Central for supplementary material.

Acknowledgments

Support for these studies was provided by the NIH (RO1CA115513, P30CA15704, UO1CA152756, U54CA143862, and P01CA077852 WMG), a Burroughs Wellcome Fund Translational Research Award for Clinician Scientist (WMG), and an Interdisciplinary Training in Cancer Research Grant (T32 CA080416 SMM).

Abbreviations

CRC	colorectal cancer
ERK	extracellular signal-regulated kinase
MAPK	mitogen-activated protein kinase
PTEN	phosphatase and tensin homolog deleted on chromosome 10
qRT-PCR	real-time quantitative reverse transcription polymerase chain reaction
TGF-β	transforming growth factor-beta
Tgfbr1	transforming growth factor-beta type I receptor
Tgfbr2	transforming growth factor-beta type II receptor
Dcr2	a decoy receptor of the TNF-related factor TRAIL

References

1. Siegel R, Naishadham D, Jemal A. Cancer statistics, 2012. CA: a cancer journal for clinicians. 62(1):10–29. [PubMed: 22237781]
2. Kinzler KW, Vogelstein B. Lessons from hereditary colorectal cancer. Cell. 1996; 87(2):159–70. Epub 1996/10/18. [PubMed: 8861899]
3. Su LK, Kinzler KW, Vogelstein B, Preisinger AC, Moser AR, Luongo C, et al. Multiple intestinal neoplasia caused by a mutation in the murine homolog of the APC gene. Science. 1992; 256(5057): 668–70. Epub 1992/05/01. [PubMed: 1350108]
4. Levy DB, Smith KJ, Beazer-Barclay Y, Hamilton SR, Vogelstein B, Kinzler KW. Inactivation of both APC alleles in human and mouse tumors. Cancer research. 1994; 54(22):5953–8. Epub 1994/11/15. [PubMed: 7954428]

5. Samowitz WS, Powers MD, Spirio LN, Nollet F, van Roy F, Slattery ML. Beta-catenin mutations are more frequent in small colorectal adenomas than in larger adenomas and invasive carcinomas. Cancer research. 1999; 59(7):1442–4. Epub 1999/04/10. [PubMed: 10197610]
6. Vogelstein B, Fearon ER, Hamilton SR, Kern SE, Preisinger AC, Leppert M, et al. Genetic alterations during colorectal-tumor development. N Engl J Med. 1988; 319(9):525–32. Epub 1988/09/01. [PubMed: 2841597]
7. Parsons DW, Wang TL, Samuels Y, Bardelli A, Cummins JM, DeLong L, et al. Colorectal cancer: mutations in a signalling pathway. Nature. 2005; 436(7052):792. [PubMed: 16094359]
8. Pritchard CC, Grady WM. Colorectal cancer molecular biology moves into clinical practice. Gut. 2011 Epub 2010/10/06.
9. Grady WM, Carethers JM. Genomic and epigenetic instability in colorectal cancer pathogenesis. Gastroenterology. 2008; 135(4):1079–99. Epub 2008/09/09. [PubMed: 18773902]
10. Jass JR. Classification of colorectal cancer based on correlation of clinical, morphological and molecular features. Histopathology. 2007; 50(1):113–30. [PubMed: 17204026]
11. Liu XQ, Rajput A, Geng L, Ongchin M, Chaudhuri A, Wang J. Restoration of transforming growth factor-beta receptor II expression in colon cancer cells with microsatellite instability increases metastatic potential in vivo. The Journal of biological chemistry. 2011; 286(18):16082–90. [PubMed: 21454688]
12. Liu P, Cheng H, Roberts TM, Zhao JJ. Targeting the phosphoinositide 3-kinase pathway in cancer. Nature Rev Drug Discov. 2009; 8:627–44. [PubMed: 19644473]
13. Luo J, Manning BD, Cantley LC. Targeting the PI3K-Akt pathway in human cancer: rationale and promise. Cancer Cell. 2003; 4(4):257–62. Epub 2003/10/31. [PubMed: 14585353]
14. Engelman JA. Targeting PI3K signalling in cancer: opportunities, challenges and limitations. Nature reviews Cancer. 2009; 9(8):550–62. Epub 2009/07/25.
15. Maehama T, Dixon JE. The tumor suppressor, PTEN/MMAC1, dephosphorylates the lipid second messenger, phosphatidylinositol 3,4,5-trisphosphate. The Journal of biological chemistry. 1998; 273(22):13375–8. [PubMed: 9593664]
16. Di Cristofano A, Pandolfi PP. The multiple roles of PTEN in tumor suppression. Cell. 2000; 100(4):387–90. [PubMed: 10693755]
17. Naguib A, Cooke JC, Happerfield L, Kerr L, Gay LJ, Luben RN, et al. Alterations in PTEN and PIK3CA in colorectal cancers in the EPIC Norfolk study: associations with clinicopathological and dietary factors. BMC Cancer. 11:123. Epub 2011/04/09. [PubMed: 21473780]
18. Zhou XP, Loukola A, Salovaara R, Nystrom-Lahti M, Peltomaki P, de la Chapelle A, et al. PTEN mutational spectra, expression levels, and subcellular localization in microsatellite stable and unstable colorectal cancers. The American journal of pathology. 2002; 161(2):439–47. [PubMed: 12163369]
19. Shin I, Bakin AV, Rodeck U, Brunet A, Arteaga CL. Transforming Growth Factor beta Enhances Epithelial Cell Survival via Akt-dependent Regulation of FKHRL1. Mol Biol Cell. 2001; 12(11): 3328–39. [PubMed: 11694570]
20. Fearon ER. Molecular genetics of colorectal cancer. Annual review of pathology. 6:479–507.
21. Song MS, Salmena L, Pandolfi PP. The functions and regulation of the PTEN tumour suppressor. Nature reviews Molecular cell biology. 2012; 13(5):283–96. Epub 2012/04/05.
22. Shen WH, Balajee AS, Wang J, Wu H, Eng C, Pandolfi PP, et al. Essential role for nuclear PTEN in maintaining chromosomal integrity. Cell. 2007; 128(1):157–70. [PubMed: 17218262]
23. Chen Z, Trotman LC, Shaffer D, Lin HK, Dotan ZA, Niki M, et al. Crucial role of p53-dependent cellular senescence in suppression of Pten-deficient tumorigenesis. Nature. 2005; 436(7051):725–30. [PubMed: 16079851]
24. Alimonti A, Nardella C, Chen Z, Clohessy JG, Carracedo A, Trotman LC, et al. A novel type of cellular senescence that can be enhanced in mouse models and human tumor xenografts to suppress prostate tumorigenesis. The Journal of clinical investigation. 2010; 120(3):681–93. Epub 2010/03/04. [PubMed: 20197621]
25. Massague J, Blain SW, Lo RS. TGF[beta] Signaling in Growth Control, Cancer, and Heritable Disorders. Cell. 2000; 103(2):295. [PubMed: 11057902]

26. Cancer Genome Atlas N. Comprehensive molecular characterization of human colon and rectal cancer. Nature. 2012; 487(7407):330–7. Epub 2012/07/20. [PubMed: 22810696]
27. Grady W, Rajput A, Myeroff L, Liu D, Kwon K-H, Willis J, et al. Mutation of the type II transforming growth factor-β receptor is coincident with the transformation of human colon adenomas to malignant carcinomas. Cancer research. 1998; 58:3101–4. [PubMed: 9679977]
28. Grady W, Myeroff L, Swinler S, Rajput A, Thiagalingam S, Lutterbaugh J, et al. Mutational inactivation of transforming growth factor β receptor type II in microsatellite stable colon cancers. Cancer research. 1999; 59:320–4. [PubMed: 9927040]
29. Bierie B, Moses HL. Tumour microenvironment: TGFbeta: the molecular Jekyll and Hyde of cancer. Nature reviews Cancer. 2006; 6(7):506–20.
30. Grady, W.; Markowitz, SD. TGF-β Signaling Pathway and Tumor Suppression. In: Derynck, R.; Miyazano, K., editors. The TGF-β Family. Cold Spring Harbor: Cold Spring Harbor Laboratory Press; 2008. p. 889-938.
31. Biswas S, Chytil A, Washington K, Romero-Gallo J, Gorska AE, Wirth PS, et al. Transforming growth factor beta receptor type II inactivation promotes the establishment and progression of colon cancer. Cancer research. 2004; 64(14):4687–92. [PubMed: 15256431]
32. Akhurst RJ, Derynck R. TGF-beta signaling in cancer--a double-edged sword. Trends in cell biology. 2001; 11(11):S44–51. [PubMed: 11684442]
33. Munoz NM, Upton M, Rojas A, Washington MK, Lin L, Chytil A, et al. Transforming growth factor beta receptor type II inactivation induces the malignant transformation of intestinal neoplasms initiated by Apc mutation. Cancer research. 2006; 66(20):9837–44. [PubMed: 17047044]
34. Trobridge P, Knoblaugh S, Washington MK, Munoz NM, Tsuchiya KD, Rojas A, et al. TGF-beta receptor inactivation and mutant Kras induce intestinal neoplasms in mice via a beta-catenin-independent pathway. Gastroenterology. 2009; 136(5):1680–8. e7. [PubMed: 19208363]
35. Marsh V, Winton DJ, Williams GT, Dubois N, Trumpp A, Sansom OJ, et al. Epithelial Pten is dispensable for intestinal homeostasis but suppresses adenoma development and progression after Apc mutation. Nature genetics. 2008; 40(12):1436–44. [PubMed: 19011632]
36. Byun DS, Ahmed N, Nasser S, Shin J, Al-Obaidi S, Goel S, et al. Intestinal epithelial-specific PTEN inactivation results in tumor formation. American journal of physiology. 2011; 301(5):G856–64. [PubMed: 21836055]
37. Chittenden TW, Howe EA, Culhane AC, Sultana R, Taylor JM, Holmes C, et al. Functional classification analysis of somatically mutated genes in human breast and colorectal cancers. Genomics. 2008; 91(6):508–11. Epub 2008/04/25. [PubMed: 18434084]
38. Lesche R, Groszer M, Gao J, Wang Y, Messing A, Sun H, et al. Cre/loxP-mediated inactivation of the murine Pten tumor suppressor gene. Genesis. 2002; 32(2):148–9. [PubMed: 11857804]
39. Yilmaz M, Christofori G. Mechanisms of motility in metastasizing cells. Mol Cancer Res. 8(5): 629–42. Epub 2010/05/13. [PubMed: 20460404]
40. Bakin AV, Tomlinson AK, Bhowmick NA, Moses HL, Arteaga CL. Phosphatidylinositol 3-kinase function is required for transforming growth factor beta-mediated epithelial to mesenchymal transition and cell migration. The Journal of biological chemistry. 2000; 275(47):36803–10. Epub 2000/09/02. [PubMed: 10969078]
41. Gomes LR, Terra LF, Wailemann RA, Labriola L, Sogayar MC. TGF-beta1 modulates the homeostasis between MMPs and MMP inhibitors through p38 MAPK and ERK1/2 in highly invasive breast cancer cells. BMC Cancer. 12:26. Epub 2012/01/21. [PubMed: 22260435]
42. Langlois MJ, Roy SA, Auclair BA, Jones C, Boudreau F, Carrier JC, et al. Epithelial phosphatase and tensin homolog regulates intestinal architecture and secretory cell commitment and acts as a modifier gene in neoplasia. Faseb J. 2009; 23(6):1835–44. [PubMed: 19168705]
43. He XC, Zhang J, Tong WG, Tawfik O, Ross J, Scoville DH, et al. BMP signaling inhibits intestinal stem cell self-renewal through suppression of Wnt-beta-catenin signaling. Nature genetics. 2004; 36(10):1117–21. [PubMed: 15378062]
44. Wielenga VJ, Smits R, Korinek V, Smit L, Kielman M, Fodde R, et al. Expression of CD44 in Apc and Tcf mutant mice implies regulation by the WNT pathway. The American journal of pathology. 1999; 154(2):515–23. Epub 1999/02/23. [PubMed: 10027409]

45. Lustig B, Jerchow B, Sachs M, Weiler S, Pietsch T, Karsten U, et al. Negative feedback loop of Wnt signaling through upregulation of conductin/axin2 in colorectal and liver tumors. Molecular and cellular biology. 2002; 22(4):1184–93. Epub 2002/01/26. [PubMed: 11809809]
46. Muncan V, Sansom OJ, Tertoolen L, Phesse TJ, Begthel H, Sancho E, et al. Rapid loss of intestinal crypts upon conditional deletion of the Wnt/Tcf-4 target gene c-Myc. Molecular and cellular biology. 2006; 26(22):8418–26. Epub 2006/09/07. [PubMed: 16954380]
47. Glick AB, Weinberg WC, Wu I-H, Quan W, Yuspa SH. TGF-β1 suppresses genomic instability downstream of a G1 arrest by a p53 and Rb independent pathway. Cell. 1996 submitted.
48. Liang J, Zubovitz J, Petrocelli T, Kotchetkov R, Connor MK, Han K, et al. PKB/Akt phosphorylates p27, impairs nuclear import of p27 and opposes p27-mediated G1 arrest. Nature medicine. 2002; 8(10):1153–60.
49. Massague J. TGFbeta in Cancer. Cell. 2008; 134(2):215–30. Epub 2008/07/30. [PubMed: 18662538]
50. Moses H, Yang E, Pietenpol J. TGF-β stimulation and inhibition of cell proliferation: new mechanistic insights. Cell. 1990; 63:245–7. [PubMed: 2208284]
51. Chu IM, Hengst L, Slingerland JM. The Cdk inhibitor p27 in human cancer: prognostic potential and relevance to anticancer therapy. Nature reviews Cancer. 2008; 8(4):253–67.
52. Abbas T, Dutta A. p21 in cancer: intricate networks and multiple activities. Nature reviews Cancer. 2009; 9(6):400–14.
53. Lee MH, Yang HY. Negative regulators of cyclin-dependent kinases and their roles in cancers. Cell Mol Life Sci. 2001; 58(12–13):1907–22. [PubMed: 11766887]
54. Shin KH, Park YJ, Park JG. PTEN gene mutations in colorectal cancers displaying microsatellite instability. Cancer letters. 2001; 174(2):189–94. Epub 2001/11/02. [PubMed: 11689295]
55. Datto MB, Yu Y, Wang XF. Functional analysis of the transforming growth factor beta responsive elements in the WAF1/Cip1/p21 promoter. The Journal of biological chemistry. 1995; 270(48): 28623–8. Epub 1995/12/01. [PubMed: 7499379]
56. Philp AJ, Campbell IG, Leet C, Vincan E, Rockman SP, Whitehead RH, et al. The phosphatidylinositol 3′-kinase p85alpha gene is an oncogene in human ovarian and colon tumors. Cancer Res. 2001; 61(20):7426–9. Epub 2001/10/19. [PubMed: 11606375]
57. Roy HK, Olusola BF, Clemens DL, Karolski WJ, Ratashak A, Lynch HT, et al. AKT proto-oncogene overexpression is an early event during sporadic colon carcinogenesis. Carcinogenesis. 2002; 23(1):201–5. Epub 2002/01/05. [PubMed: 11756242]
58. Byun DS, Ahmed N, Nasser S, Shin J, Al-Obaidi S, Goel S, et al. Intestinal epithelial-specific PTEN inactivation results in tumor formation. Am J Physiol Gastrointest Liver Physiol. 301(5):G856–64. Epub 2011/08/13. [PubMed: 21836055]
59. Stambolic V, Suzuki A, de la Pompa JL, Brothers GM, Mirtsos C, Sasaki T, et al. Negative regulation of PKB/Akt-dependent cell survival by the tumor suppressor PTEN. Cell. 1998; 95(1): 29–39. [PubMed: 9778245]
60. Leystra AA, Deming DA, Zahm CD, Farhoud M, Olson TJ, Hadac JN, et al. Mice expressing activated PI3K rapidly develop advanced colon cancer. Cancer research. 2012; 72(12):2931–6. Epub 2012/04/25. [PubMed: 22525701]
61. Grady WM, Willis JE, Trobridge P, Romero-Gallo J, Munoz N, Olechnowicz J, et al. Proliferation and Cdk4 expression in microsatellite unstable colon cancers with TGFBR2 mutations. International journal of cancer. 2006; 118(3):600–8.
62. Jaiswal BS, Janakiraman V, Kljavin NM, Chaudhuri S, Stern HM, Wang W, et al. Somatic mutations in p85alpha promote tumorigenesis through class IA PI3K activation. Cancer Cell. 2009; 16(6):463–74. Epub 2009/12/08. [PubMed: 19962665]
63. Panopoulou E, Murphy C, Rasmussen H, Bagli E, Rofstad EK, Fotsis T. Activin A suppresses neuroblastoma xenograft tumor growth via antimitotic and antiangiogenic mechanisms. Cancer Res. 2005; 65(5):1877–86. Epub 2005/03/09. [PubMed: 15753386]
64. Jung B, Doctolero RT, Tajima A, Nguyen AK, Keku T, Sandler RS, et al. Loss of activin receptor type 2 protein expression in microsatellite unstable colon cancers. Gastroenterology. 2004; 126(3): 654–9. Epub 2004/02/28. [PubMed: 14988818]

65. Bauer J, Sporn JC, Cabral J, Gomez J, Jung B. Effects of activin and TGFbeta on p21 in colon cancer. PloS one. 2012; 7(6):e39381. Epub 2012/07/05. [PubMed: 22761777]

66. Chen CN, Lin JJ, Chen JJ, Lee PH, Yang CY, Kuo ML, et al. Gene expression profile predicts patient survival of gastric cancer after surgical resection. J Clin Oncol. 2005; 23(29):7286–95. [PubMed: 16145069]

67. Collado M, Gil J, Efeyan A, Guerra C, Schuhmacher AJ, Barradas M, et al. Tumour biology: senescence in premalignant tumours. Nature. 2005; 436(7051):642. [PubMed: 16079833]

68. Young LC, Listgarten J, Trotter MJ, Andrew SE, Tron VA. Evidence that dysregulated DNA mismatch repair characterizes human nonmelanoma skin cancer. The British journal of dermatology. 2008; 158(1):59–69. [PubMed: 17970804]

69. Majumder PK, Grisanzio C, O'Connell F, Barry M, Brito JM, Xu Q, et al. A prostatic intraepithelial neoplasia-dependent p27 Kip1 checkpoint induces senescence and inhibits cell proliferation and cancer progression. Cancer cell. 2008; 14(2):146–55. [PubMed: 18691549]

70. Ise K, Nakamura K, Nakao K, Shimizu S, Harada H, Ichise T, et al. Targeted deletion of the H-ras gene decreases tumor formation in mouse skin carcinogenesis. Oncogene. 2000; 19(26):2951–6. Epub 2000/06/29. [PubMed: 10871846]

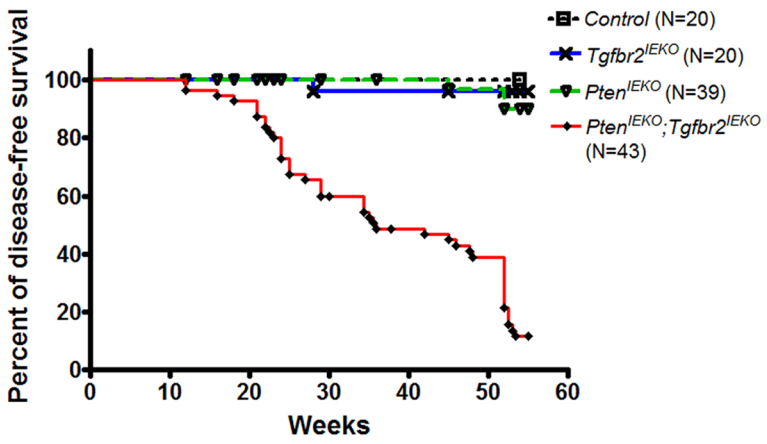

Figure 1. Inactivation of Tgf-β signaling and loss of *Pten* lead to markedly reduced survival

Kaplan-Meier analysis reveals a median survival of 36 weeks in $Pten^{IEKO};Tgfbr2^{IEKO}$ mice (N=43). A significant decrease in the survival of $Pten^{IEKO};Tgfbr2^{IEKO}$ mice was observed compared to $Tgfbr2^{IEKO}$ mice, $Pten^{IEKO}$ mice or Control mice ($P < 0.0001$, log-rank test, for all comparisons). There was no significant difference in survival when the $Tgfbr2^{IEKO}$ mice or $Pten^{IEKO}$ mice were compared to Control mice ($P > 0.1$ for both comparisons, log-rank test). Of note, all mice that survived to 54 weeks of age were sacrificed at that age.

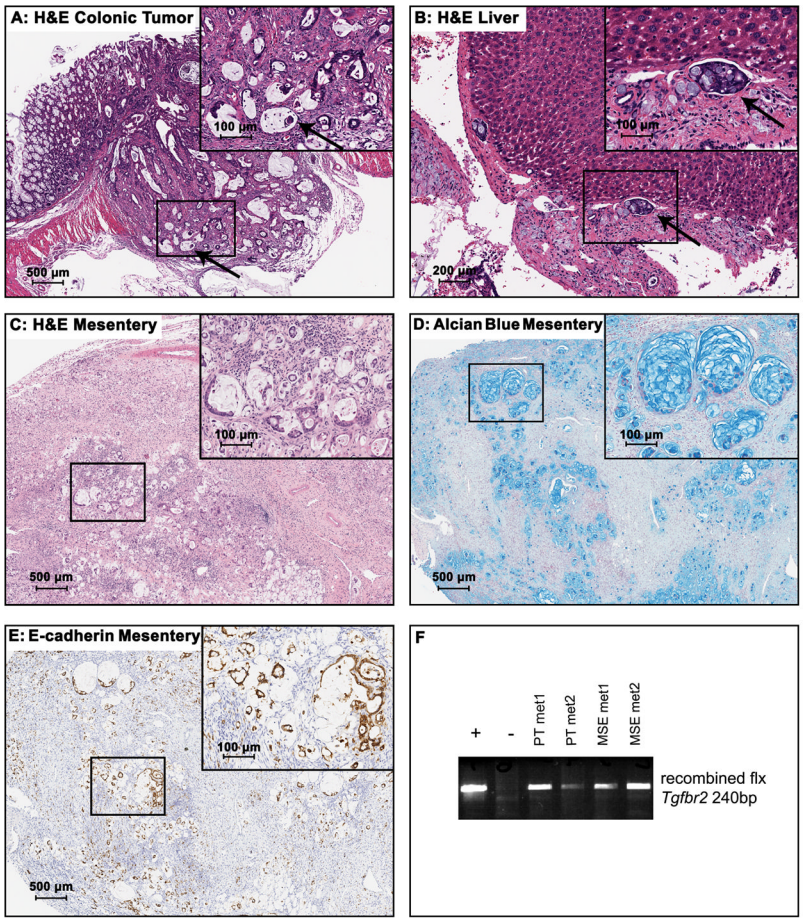

Figure 2. Inactivation of Tgf-β signaling and loss of *Pten* lead to formation of invasive adenocarcinomas

(A) Low-power image of a representative colonic mucinous adenocarcinoma from a $Pten^{IEKO};Tgfbr2^{IEKO}$ mouse (H&E, original magnification: 20X). There is transmural effacement by neoplastic glands and large lakes of tumor-produced mucin. In some cases, mucin lakes extend through the serosa and into the serosal lymphatics. The inset was taken from the boxed region in (A) at higher magnification and the arrow points to intravascular neoplastic cells within the primary colonic mucinous adenocarcinoma (H&E, original magnification: 200X). (B) Low-power image of a liver section reveals intravascular neoplastic cells (H&E, original magnification: 100X). The inset was taken from the boxed region in (B) at higher magnification and the arrow points to the intravascular neoplastic cells (H&E, original magnification, 200X). (C) Low-power image of a mesenteric metastasis arising from a $Pten^{IEKO};Tgfbr2^{IEKO}$ mouse (H&E, original magnification: 40X). The inset was taken from the boxed region in (C) at higher magnification to show the neoplastic glands and mucin production (H&E, original magnification: 200X). (D) Low-power image of Alcian blue stained section of the same mesenteric metastasis shown in panel C (Alcian blue stain, original magnification: 40X). The inset was taken from the boxed region in (D) at higher magnification to show the mucin production in this metastasis (Alcian blue stain, original magnification: 200X). (E) E-cadherin immunostaining of the same mesentery metastasis shown in (C) (E-cadherin IHC, original magnification: 40X). The inset was taken from the boxed region in (E) at higher magnification to demonstrate strong expression of E-cadherin, consistent with the epithelial origin of this metastasis (original magnification: 200X). (F) PCR genotyping results demonstrate the recombination of the $Tgfbr2^{flx}$ allele in

peritoneal metastasis (PT met1 and PT met2) and mesentery metastases (MSE met1 and MSE met2). The positive control DNA is from the small intestine mucosa of a *Tgfbr2*$^{IE\text{KO}}$ mouse, and the negative control DNA is from the lymph nodes of a *Pten*^{IEKO};*Tgfbr2*$^{IE\text{KO}}$ mouse that did not have grossly evident metastatic disease.

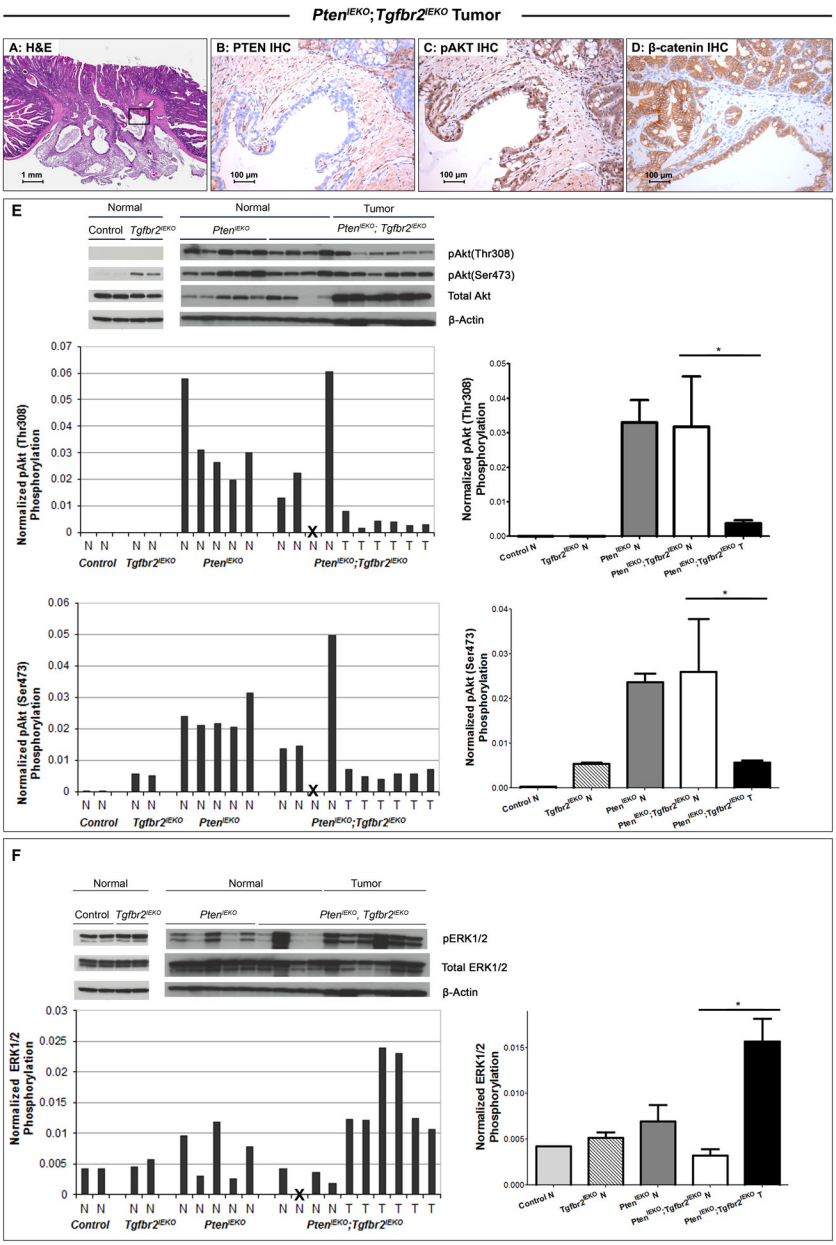

Figure 3. Signaling pathway deregulation in *Pten^{IEKO};Tgfbr2^{IEKO}* tumors

(A) Low-power image of a representative intestinal adenocarcinoma from a *Pten^{IEKO};Tgfbr2^{IEKO}* mouse (H&E, original magnification: 20X). The boxed region in (A) is shown at higher magnification in the adjacent photomicrographs of immunostained tissue. Neoplastic epithelial cells in *Pten^{IEKO};Tgfbr2^{IEKO}* mice show (A) decreased PTEN expression by PTEN immunostaining and (B) increased Akt activation by phospho-Akt (Ser473) immunostaining. The invasive front of a representative adenocarcinoma shows (C) membrane-bound β-catenin. (A–C, original magnification 200X). (D) Upper level, analysis of activation of Akt by immunoblotting of lysates from normal mucosa of wild-type (WT) control and *Tgfbr2^{IEKO}* mice (left panel); in normal mucosa of *Pten^{IEKO}* mice, normal mucosa and tumors from *Pten^{IEKO};Tgfbr2^{IEKO}* mice (right panel). β-actin was used as a loading control. Middle level and lower level, relative Akt phosphorylation levels at Thr308

and Ser473 sites as determined by densitometry, normalized to total Akt and further normalized to β-actin. Note a significant decrease in relative Akt phosphorylation levels at Thr308 and Ser473 sites in tumors tissue (T) compared to normal tissue (N) from $Pten^{IEKO};Tgfbr2^{IEKO}$ mice. (* $p<0.05$ for both relative pAkt T308 and S473, Mann-Whitney test) (E) Upper level, analysis of activation of ERK1/2 by immunoblotting of lysates from normal mucosa of wild-type Control and $Tgfbr2^{IEKO}$ mice (left panel); in normal mucosa of $Pten^{IEKO}$ mice, normal mucosa and tumors from $Pten^{IEKO};Tgfbr2^{IEKO}$ mice (right panel). β-actin was used as a loading control. Lower level, relative ERK1/2 phosphorylation levels as determined by densitometry, normalized to total ERK1/2 and further normalized to β-actin. Note a significant increase in relative ERK1/2 phosphorylation levels in tumor tissue (T) compared to normal tissue (N) from $Pten^{IEKO};Tgfbr2^{IEKO}$ mice. (* $p<0.05$, Mann-Whitney test).

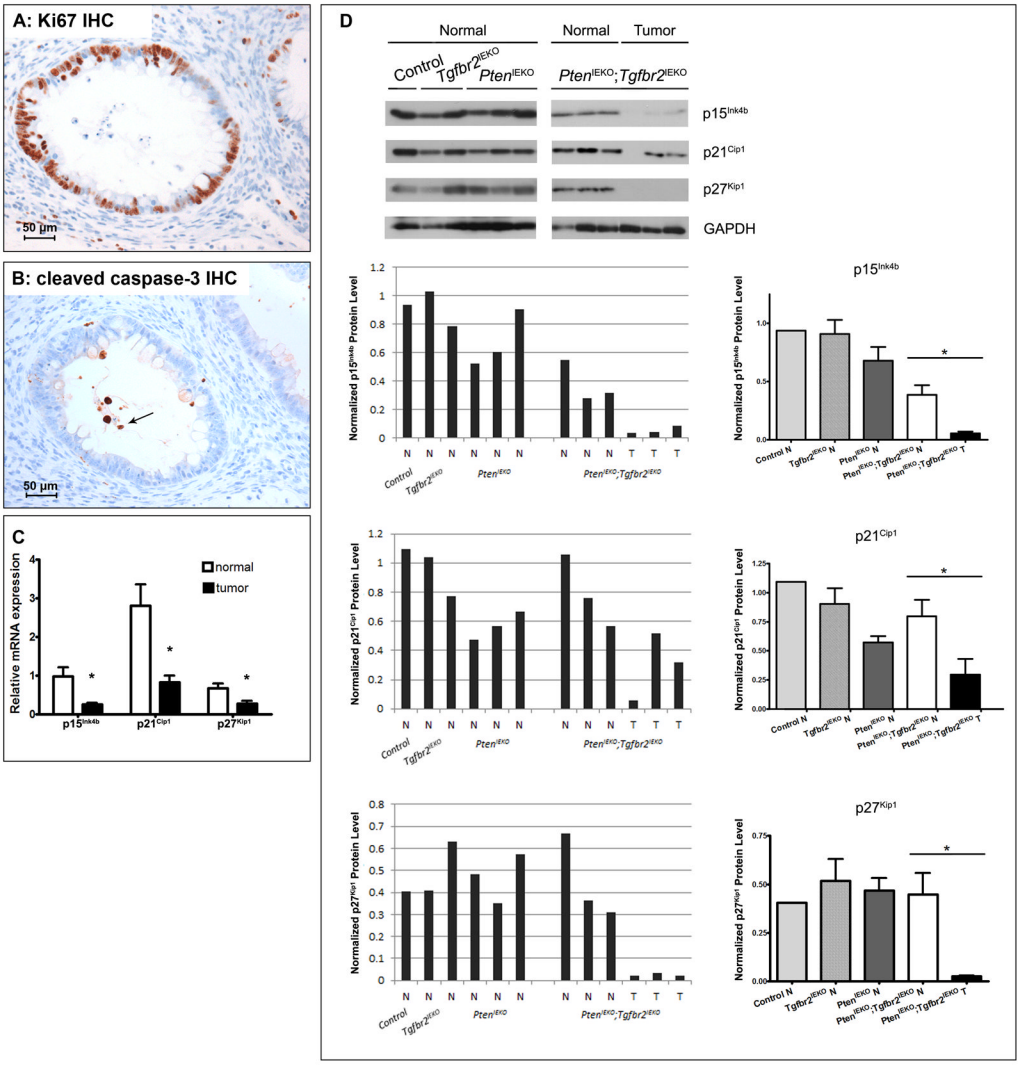

Figure 4. Assessment of proliferation, apoptosis and cyclin dependent kinase inhibitors in normal tissue and *Pten^{IEKO};Tgfbr2^{IEKO}* tumors

(A) Representative photomicrograph of Ki67 immunostained tumor from *Pten^{IEKO};Tgfbr2^{IEKO}* mice. (B) Representative photomicrograph of cleaved caspase-3 immunostained tumor from *Pten^{IEKO};Tgfbr2^{IEKO}* mice. Rare stained cells are present and stained cellular debris is noted within the lumen of neoplastic glands (arrow). (C) Assessment of *p15^{Ink4b}* (*Cdkn2b*), *p21^{Cip1}* (Cdkn1a) and *p27^{Kip1}*(*Cdkn1b*) mRNA by qRT-PCR in matched normal mucosa and tumors from *Pten^{IEKO};Tgfbr2^{IEKO}* mice. (Mann-Whitney test, * p=0.01 for *p15^{Ink4b}*(*Cdkn2b*), 0.0033 for *p21^{Cip1}(Cdkn1a)*, and 0.015 for *p27^{Kip1}*(*Cdkn1b*)) (D) Assessment of p15^{Ink4b}, p21^{Cip1} and p27^{Kip1} protein levels by immunoblotting lysates from normal mucosa of various genotypes, and normal mucosa and tumors from the *Pten^{IEKO};Tgfbr2^{IEKO}* mice. GAPDH was used as a loading control. Normalized protein levels of p15^{Ink4b}, p21^{Cip1} and p27^{Kip1} were determined by densitometry, normalized to GAPDH. Note a significant decrease in normalized levels of p15^{Ink4b}, p21^{Cip1} and p27^{Kip1} in tumor tissue (T) compared to normal tissue (N) from *Pten^{IEKO};Tgfbr2^{IEKO}* mice. (* p<0.05, Mann-Whitney test, N=3)

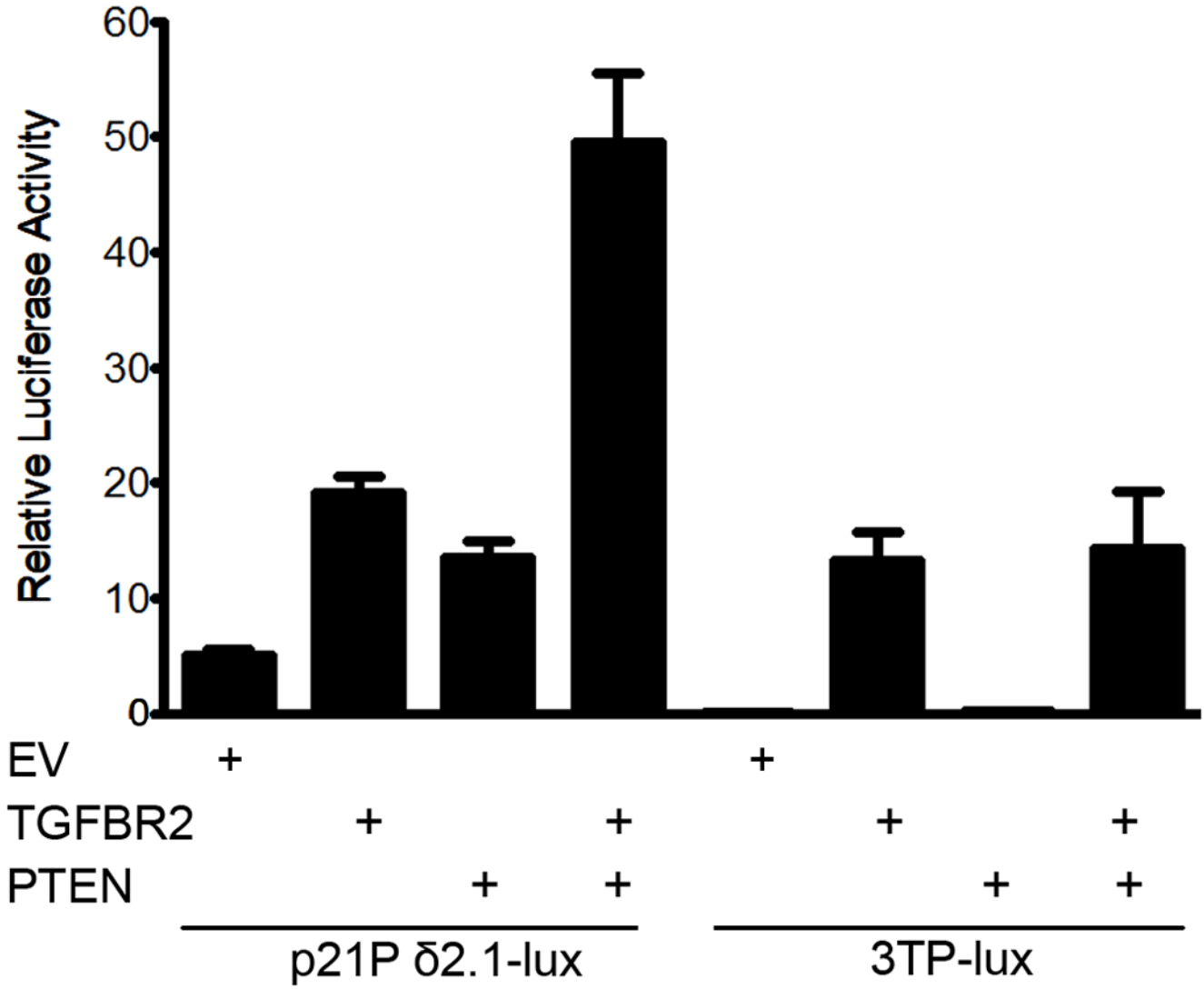

Figure 5. Reconstitution of *TGFBR2* and *PTEN* induce $p21^{CIP1}$ expression in colon cancer cells

Stimulation of p21Pδ2.1 reporter luciferase activity in the colon cancer cell line SNU-C4 transfected with empty vector (EV), *TGFBR2*, *PTEN*, or both *TGFBR2* and *PTEN*. Transfected SNU-C4 cells were treated with TGF-β (2 ng/ml). Histograms represent relative luciferase activity normalized to Renilla luciferase reporter activity. The error bars represent the standard error from three independent experiments. The 3TP-lux luciferase reporter was used to confirm the specificity of the cooperation between *TGFBR2* and *PTEN* on the activation of $p21^{CIP1}$ luciferase reporter. Reconstitution of the SNU-C4 cells with *PTEN* alone did not induce 3TP-lux activity. Furthermore, there was no increase in the luciferase activity of the 3TP-lux reporter in *TGFBR2* and *PTEN* co-transfected cells compared to *TGFBR2*-transfected alone cells, indicating the specificity of the additive effect of *PTEN* and *TGFBR2* on $p21^{CIP1}$ expression.

Table 1

Tumor incidence in Control, *Tgfbr2*^{IEKO}, *Pten*^{IEKO} and *Pten*^{IEKO};*Tgfbr2*^{IEKO} mice

Genotype	Number of mice	Number of mice with hyperplastic lesions	Number of mice with adenocarcinomas	Number of hyperplastic lesions	Number of adenocarcinomas
Control[#]	20	0	0	0	0
Tgfbr2^{IEKO}	20	0	0	0	0
Pten^{IEKO}	39	2[€]	1[λ]	3	1
Pten^{IEKO}; *Tgfbr2*^{IEKO}	43	4[μ,£,¥]	35[δ,&,¥]	4	49

[#]Control = wild-type mice, matched strain background

[€]$P = 0.54$, *Pten*^{IEKO} (2/39) vs. Control (0/20), Fisher's exact test

[λ]$P = 1.0$, *Pten*^{IEKO} (1/39) vs. Control (0/20), Fisher's exact test

[μ]$P = 0.30$, *Pten*^{IEKO}; *Tgfbr2*^{IEKO} (4/43) vs. Control (0/20), Fisher's exact test

[£]$P = 0.68$, *Pten*^{IEKO}; *Tgfbr2*^{IEKO} (4/43) vs. *Pten*^{IEKO} (2/39), Fisher's exact test

[δ]$P < 0.0001$, *Pten*^{IEKO}; *Tgfbr2*^{IEKO} (35/43) vs. Control (0/20), Fisher's exact test

[&]$P < 0.0001$, *Pten*^{IEKO}; *Tgfbr2*^{IEKO} (35/43) vs. *Pten*^{IEKO} (1/39), Fisher's exact test

[¥]N=2 mice developed one adenocarcinoma and one hyperplastic lesion with dysplasia

Table 2

Anatomic distribution of adenocarcinomas in *Pten*^{IEKO};*Tgfbr2*^{IEKO} mice

Genotype	Number of ACA	Small Intestine	Cecum	Colon	Cecal Junction
Pten^{IEKO}; *Tgfbr2*^{IEKO}	49	16 (32.7%)	11(22.4%)	13(26.5%)	9(18.4%)